Ecological Modelling, 49 (1989) 101–124
Elsevier Science Publishers B.V., Amsterdam – Printed in The Netherlands

MODEL OF THE SEASONAL AND PERENNIAL CARBON DYNAMICS IN DECIDUOUS-TYPE FORESTS CONTROLLED BY CLIMATIC VARIABLES

A. JANECEK, G. BENDEROTH, M.K.B. LÜDEKE, J. KINDERMANN and G.H. KOHLMAIER

Institut für Physikalische und Theoretische Chemie, Johann Wolfgang Goethe Universität Frankfurt, Niederurseler Hang, 6000 Frankfurt 50 (Federal Republic of Germany)

(Accepted 24 May 1989)

ABSTRACT

Janacek, A., Benderoth, G., Lüdeke, M.K.B., Kindermann, J. and Kohlmaier, G.H., 1989. Model of the seasonal and perennial carbon dynamics in deciduous-type forests controlled by climatic variables. *Ecol. Modelling*, 49: 101–124.

A model of the seasonal and long-term carbon dynamics of temperature deciduous forests and tropical broadleaved evergreen forests in response to variations of the climatic parameters light intensity and air temperature, is proposed in order to be able to assess the influence of (future) climatic change on vegetation. The driving variables operate upon carbon assimilation and respiration of a two-compartment model of living biomass. The model allocation of assimilates depends on the developmental stage of the living biomass and on the climatic variables, without prescribing the time course of the phenophases explicitly. Almost all model parameters can be interpreted in terms of measurable physiological/ecological quantities, restricting the parameter values to a limited range. Measured growth dynamics and annual CO_2 fluxes for a non-seasonal tropical forest and two different temperate deciduous forest stands are reproduced satisfactorily.

1. INTRODUCTION

Global warming as a consequence of anthropogenic emissions of CO_2 and other trace gases seems almost inevitable. Predictions of the future greenhouse climate emphasize considerable changes in the regional and seasonal patterns of, e.g., surface temperature, precipitation and cloud cover. Vegetation will certainly respond to these changes and influence the climatic development in a feed-back loop (e.g. changes in the carbon cycle, energy budget and albedo). Solomon (1986) presented a detailed study of the transient response of North American forests to future $2\times$ and $4\times CO_2$ climates, where growth, establishment and mortality of mixed-species and mixed-age stands was simulated stochastically. The model used was a complex stand model which needs a broad variety of stand-specific informa-

0304-3800/89/$03.50

tion and thus cannot be applied to global-scale processes in a reasonable manner. King et al. (1987), employing the Monte Carlo method in order to account for the nonlinear model response to the vast variety of driving variables, attempted to adapt to global biomes eight different stand-specific models from the literature, and succeeded in simulating the seasonal carbon uptake and release in the latitude belt between 60 and 90 °N, which is constituted of tundra and boreal forests. This approach also seems to be too complicated for global-scale modelling; its major disadvantage lies in the very heterogeneous and interdependent driving-parameter sets, such that runs with predicted climate from global circulation models are hardly feasible. On the other hand there are, mostly from carbon cycle modellers, quite simplistic seasonal models of the global biosphere activity, using, e.g., a correlation between monthly mean temperature and seasonal CO_2 source/sink function (Pearman and Hyson, 1986).

We present here a first step towards a model in between: simple enough to be employed on a global scale, but allowing for an adaption to different vegetation units and local climatic events, neglecting any migration phenomena. As driving variables, only light intensity and surface air temperature are used. The ecosystems considered here are the temperate deciduous forest, as it exhibits the most pronounced seasonality, and as a contrast, the evergreen tropical moist forest.

2. MODEL DESCRIPTION

Only the living part of the terrestrial vegetation shall be considered here, as carbon assimilation in response to climatic variables is the primary measure of its activity. For seasonal carbon-cycle modelling purposes it can be readily amplified by a litter-decomposition module as given, e.g., by Fung et al. (1987).

2.1. Compartments

Considering the different functional elements of annual (herbaceous), and in particular perennial plants (trees), in the deciduous-forest ecosystem type, the following classification, with respect to the seasonal mass fluctuation, can be made:

Pronounced mass fluctuation	Relatively small mass fluctuation
Photosynthesizing tissues	Stems
Assimilate store	Branches
Feeder roots	Woody roots
Flowers	
Fruits	

The different behaviour of these functional elements requires a subdivision of the living biomass into at least two compartments. Here, especially the separation of the photosynthetic tissue from the non-productive woody parts with a relatively small seasonal fluctuation seems important. The following subdivision is proposed:

(1) green photosynthesizing biomass, assimilate store and feeder roots, summarized by the compartment G (green biomass);
(2) remaining biomass, consisting mainly of woody parts, summarized by the compartment R (remaining biomass).

Flowers and fruits are not considered in this approach due to their negligible biomass. The seasonally fluctuating feeder-root biomass constitute an amount comparable to the leaf biomass and closely follows the dynamics of the photosynthetic tissue, since its growth is controlled by the leaf biomass, induced by its demand for water and nutrients. Here we shall assume a constant proportion between feeder roots and green plant material, depending on the vegetation type.

In the case of deciduous forests, compartment G is assumed to represent also an effective assimilate store for the shoot in spring. This storage part of

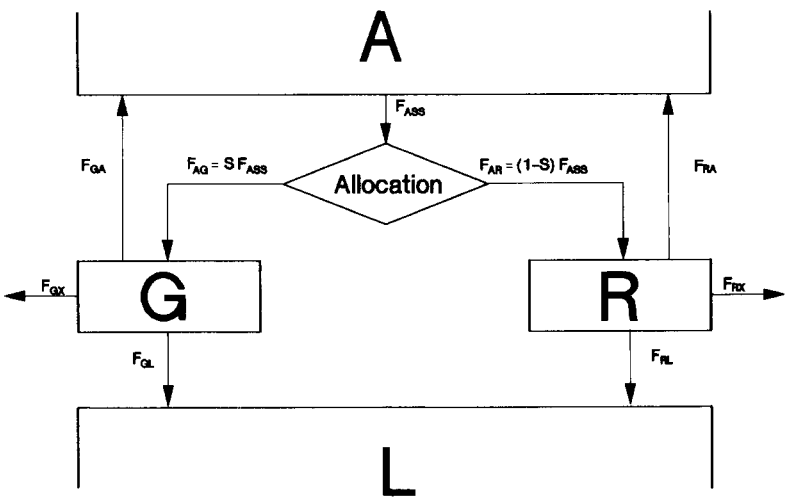

Fig. 1. Flow diagram. The big capital letters represent the reservoirs: A, atmosphere; G, green biomass; R, remaining biomass; L, litter. The capital letters F represent carbon fluxes where the first letter of the subscript indicates the donor and the second the acceptor compartment, except of the carbon assimilation rate: F_{ASS} carbon assimilation rate, F_{AG} fraction of F_{ASS} allocated into the G-compartment, F_{AR} fraction of F_{ASS} allocated into the R-compartment, F_{GA} autotroph respiration of the G-compartment, F_{RA} autotroph respiration of the R-compartment, F_{GX} other carbon losses of the G-compartment, F_{RX} other carbon losses of the R-compartment, F_{GL} litter production of the G-compartment, F_{RL} litter production of the R-compartment.

G compartment could potentially allow for a non-realistic, enhanced photosynthetic carbon uptake: during the vegetation period this extra contribution can be compensated by a smaller effective maximum photosynthesis rate, whereas at reduced temperature and light intensity during winter the resulting production rate is very small, and essentially compensated by respiration losses, keeping the assimilate-store biomass approximately constant during this period.

This minimal division of the living biomass into two compartments seems to be sufficient and practicable with respect to the actual aim of describing global vegetation dynamics, especially considering the fact that little is known about allocation into a more-differentiated compartmentization at the ecosystem level. In Fig. 1 we show a carbon-flow diagram for the two compartments G and R as connected to the atmosphere A and litter pool L. The carbon fluxes between the individual compartments are designated by the capital letter F and, in general, a two-letter subscript (donor–acceptor compartment), explained in the legend of Fig. 1. Fundamental to our approach of the seasonal assimilate allocation is the introduction of a switching function S, which partitions primary production between the compartments G and R, as explained in detail in Section 2.5. The flowchart is representative of the following set of differential equations:

$$\mathrm{d}G/\mathrm{d}t = S(G, R, I, T)\, F_{\mathrm{ASS}}(G, I, T) - F_{\mathrm{GA}}(G, T) - F_{\mathrm{GL}}(G, D) - F_{\mathrm{GX}}(G) \quad (1)$$

$$\mathrm{d}R/\mathrm{d}t = (1 - S(G, R, I, T))\, F_{\mathrm{ASS}}(G, I, T) - F_{\mathrm{RA}}(R, T) - F_{\mathrm{RL}}(R) - F_{\mathrm{RX}}(R) \quad (2)$$

where S is the fraction of the total assimilate flux F_{ASS} that enters into G, while $(1 - S)$ is the fraction entering into R ($0 \leqslant S \leqslant 1$). Light intensity I, temperature T and daylength D are all functions of time t, which describes the particular hour and day of the year.

2.2. Assimilation of carbon in its seasonal pattern

The most important factors influencing carbon assimilation, F_{ASS}, are the photosynthetically active radiation per leaf area (PAR), ambient temperature T, water availability (soil moisture), ambient CO_2 concentration, and nutrient supply. These external factors show a more-or-less seasonal variation, and induce a corresponding fluctuation in the uptake of atmospheric CO_2. In this first model approach, only the temperature (T) and light intensity (I) will be considered, since the realistic modelling of the dependence on water availability and nutrients requires a detailed submodel of the water

budget (to be dealt with in a future publication). Dependence on the ambient CO_2 concentration, which reflects the CO_2 fertilization effect of vegetation, has already been discussed in other papers (e.g. Kohlmaier et al., 1987) and can be implemented easily for carbon-cycle modelling.

The coupling of the incident light intensity with the leaf area index of the vegetation (LAI) and the effect of temperature on the annually varying flux of assimilation rate F_{ASS} shall be described by a product approach (Richter, 1985):

$$F_{ASS} = h_1(\text{LAI}, I)\, h_2(T) \tag{3}$$

2.3.1. Dependence of the assimilation rate on light intensity and leaf area index

By analogy to a simple enzymatic reaction, the dependence of the rate of photosynthesis per unit leaf area on the actual light intensity (PAR) can be modelled by a Michaelis–Menten type approach (Gates, 1980):

$$h_0(I) = P_m \frac{I(t)}{K_I + I(t)} \tag{4a}$$

where K_I is the specific Michaelis–Menten constant (see Table 1), $I(t)$ light intensity, and P_m maximum assimilation rate per unit leaf area. This relation holds for a single leaf layer.

TABLE 1

Parameters independent of ecosystem type

(a) Production			
Michaelis–Menten constant for light dependence [a]	K_I	1.5×10^2	$\frac{W}{m^2}$
Temperature dependence coefficients [a]	c	6.09×10^5	K^{-1}
	$\Delta H_\#$	4.85×10^4	$\frac{J}{mol}$
	ΔH_1	1.76×10^5	$\frac{J}{mol}$
	ΔS	5.57×10^2	$\frac{J}{K\,mol}$
(b) Autotroph respiration			
Temperature dependence parameters [b]	ω	6.0×10^{-2}	K^{-1}
	τ	317	K

[a] Derived from Gates, 1980.

[b] Derived from Lommen et al., 1971.

In an ecosystem canopy, several leaf layers shade each other, such that the actual light intensity penetrating the canopy, decreases with increasing cumulative LAI, with each leaf-area layer absorbing a certain amount of light. This fact can be described by the Lambert–Beer law. Accounting for the light attenuation, integration of equation (4a) over all leaf-layer yields, according to the model of Monsi and Saeki (1953):

$$h_1(I, \text{LAI}) = \frac{P_m}{k} \ln \frac{K_I + I(t)}{K_I + I(t)\, e^{-k\text{LAI}}} \tag{4b}$$

where k is the extinction coefficient of a single leaf-layer. Leaf area and leaf carbon mass can be related to each other for a determined ecosystem by a conversion factor u, averaging the area to mass relation of light and shade-adapted leaves and neglecting any anatomical changes during plant development from the seedling to the climax state:

$$\text{LAI} = uG \tag{4c}$$

2.3.2. Dependence of the assimilation rate on temperature

The functional form of the temperature dependence can be derived from the consideration of the reaction kinetics of photosynthesis. The essential temperature-dependent processes are the dark reaction of the Calvin cycle and the degradation and inactivation of the enzyme system. Johnson et al. (1954) found the following expression, valid also for complex plant physiological processes:

$$h_2(T) = \frac{cT\, e^{-\Delta H_\# /(RT)}}{1 + e^{-\Delta H_1/(RT)}\, e^{\Delta S/R}} \tag{5}$$

where T is the leaf temperature (K), $\Delta H_\#$ activation energy of photosynthesis, ΔH_1 activation energy of degradation, ΔS entropy of degradation, c a constant and, R the gas constant. This relation has been used successfully in modelling the temperature dependence of single-leaf photosynthesis by, e.g., Lommen et al. (1971). Under the approximation that leaf temperature equals the temperature of the surrounding air it can be used to describe the carbon assimilation rate of forest ecosystems (parameter values are given in Table 1).

2.4. Seasonal pattern of carbon losses

All carbon dissimilation and litter production rates except the autotroph respiration of the R compartment have been assumed to be proportional to the first power of the mass of the releasing compartment (donor-controlled),

with a constant or time-dependent (light incidence, temperature) rate coefficient.

2.4.1. Autotrophic respiration

Autotrophic (dark) respiration is modelled as a function of temperature (Gates, 1980). For both compartments, G and R, the relative temperature-dependence $f(T)$ of the dark respiration rate was obtained determining the parameters ω and τ (see Table 1) by fitting a quasi-Arrhenius type curve to the data used by Lommen et al. (1971):

$$f(T) = e^{\omega(T(t)-\tau)} \tag{6a}$$

Similar results were obtained by, e.g., Esser (1989). Thus the autotroph respiration of the G compartment takes the form:

$$F_{GA} = a_{GA}\, f(T)\, G \tag{6b}$$

with a_{GA} constant. The 'ecological' assumption was made that photorespiration during the day is roughly of the same magnitude as the dark respiration during the night, as proposed by, e.g., Mitscherlich (1975), such that dark respiration is operative 24 h per day for the model leaves.

For the R compartment it was assumed that only a part of its mass is involved in the process of autotroph respiration, and that the ratio of living respiring wood R_R to the dead supporting wood decreases with increasing total R mass. For the description of the fraction of metabolizing wood, R_R, the following empirical expression was chosen:

$$R_R(R) = (R + \phi)^{\gamma} - \psi \tag{7a}$$

The parameters ϕ, γ and ψ can be obtained using the condition:

$$R_R(0) = 0 \tag{7b}$$

and two typical values for the actively respiring wood fraction (Strasburger, 1985). The autotroph respiration of the R compartment then takes the form:

$$F_{RA} = a_{RA}\, f(t)\, R_R(R) \tag{8}$$

with a_{RA} constant.

2.4.2. Litter production

The flux of dead biomass into the litter compartment (litter production) is due to a series of complex variables such as physiological state, phenology, climate etc. For the woody litter production it is assumed that its mostly external causes are stochastic and add up to a more or less constant rate, b_{RL}, for larger areas, such that:

$$F_{RL} = b_{RL} R \tag{9}$$

Similarly, a constant leaf-litter production rate, b_{GL1}, is assumed for the G compartment. In the case of decidous forests an additional leaf-abscission coefficient, $b_{GL2}(t)$, is introduced, which is taken to be a function of the daylength D, assuming a photoperiodic control of this process (Strasburger, 1985; Čestnych and Gil'manov, 1986). Here it is parametrized by a Gaussian-type function, which produces a steep leaf-litter peak, described by suitable values for the fitting parameters α and ϵ, if a critical daylength ξ is reached:

$$b_{GL2}(t) = \alpha \, e^{-\epsilon(D(t)-\xi)^2} \tag{10a}$$

The leaf-litter production results in:

$$F_{GL} = b_{GL}(t) \, G \tag{10b}$$

with

$$b_{GL}(t) = \begin{cases} b_{GL1} + b_{GL2}(t) & \text{if} \quad dD/dt < 0 \\ b_{GL1} & \text{otherwise} \end{cases} \tag{10c}$$

The constant rate coefficients b_{GL1} and b_{RL} were determined using annual litter-production rates given in the literature (see Section 3).

2.4.3. Other carbon losses

A variety of additional biotic and abiotic processes lead to biomass losses by the living primary producers. The decomposition of biomass in the grazing food-chain depends not only on the standing biomass, but also on the population dynamics of the herbivores; as this process, on the average, contributes only about 5% to the total carbon turnover in the forest ecosystems, we make the simplifying assumption of constant rate-coefficients d_{GX} and d_{RX}, taken to sum up to 0.05 year^{-1} in all ecosystems considered. Other external stochastic processes such as wild-fires and plant diseases can be included in this flux, but are neglected here. The corresponding fluxes result in:

$$F_{GX} = a_{GX} G \tag{11a}$$

and

$$F_{RX} = b_{RX} R \tag{11b}$$

2.5. Assimilate allocation

As shown in Fig. 1 it is assumed that the assimilate production F_{ASS} is determined by the mass of compartment G and by the external parameters

light intensity I and temperature T. This flux is to be distributed according to the present needs of the plant organs, namely the build-up and maintenance of the photosynthesizing tissue and of the feeder roots (represented by G) on the one hand and the build-up and maintenance of stems, branches and roots (represented by R) on the other. Furthermore, assimilates have to be translocated in order to fill particular storage organs, which also are contained in the C-mass of the G compartment. It is assumed here that at any time t of plant development a given amount $R(t)$ can support and maintain maximally a determinate corresponding amount of $G(t)$. This upper boundary shall be described by the curve $\Omega^{-1}(R)$; for practical reasons the inverse function $\Omega(G)$ is used in the following.

2.5.1. Allometric relation

Up to now it has not been possible to determine the ecosystem-dependent function $\Omega(G)$ by ab-initio methods, due to the complexity of the problem. Some authors, e.g. Oikawa (1985), propose constant rates for the assimilate distribution to different plant compartments, where the trajectory in the phase space spanned by two compartments, i.e. the boundary curve $\Omega(G)$ in our case, is represented by a straight line. This description contradicts basic observation data, which in nearly all cases show a non-linear relationship between different plant compartments and also some theoretical considerations: in general, each individual compartment follows an intrinsic, non-linear growth law with a different growth rate. It can be shown mathematically (Rosen, 1967) that the trajectory in the phase space must then obey the (nonlinear) allometric relation, which describes the relative growth of different compartments of a system and has been confirmed empirically in many fields of biology (Bertalanffy et al., 1977). The allometric relation:

$$R(G) = \theta G^{\beta} \tag{12a}$$

shall be used to describe the relation between the maximum mass of G and the mass of R – the boundary $\Omega(G)$ – determining the parameters θ and β for different vegetation units by least-squares fitting to empirical data from the literature without consideration of the age structure. In lack of more-specific data it is proposed to use one fitted $\Omega(G)$ for each vegetation unit considered, neglecting possible local variations. Furthermore, the parameter θ is related to the steady-state (climax) biomass R_0 and G_0 by:

$$\theta = \frac{R_0}{G_0^{\beta}} \tag{12b}$$

2.5.2. Modelling the allocation

In order to partition the carbon assimilation rate F_{ASS} between the G and R compartment, a switching function S is defined:

$$dG/dt = SF_{ASS} - F_{G,efflux} \tag{13}$$

$$dR/dt = (1 - S)F_{ASS} - F_{R,efflux} \tag{14}$$

where $F_{G,efflux}$ and $F_{R,efflux}$ denote the sum of the effluxes from the G or R compartment, respectively; S is restricted to the range $0 \leqslant S \leqslant 1$ to ensure that F_{ASS} is exactly distributed. S will not determine the system dynamics in advance and is therefore modelled as a function of the state of the system in the G–R plane (phase-space controlled). No explicit time-switches will be used.

2.5.3. Determination of the switching function for tropical rain forests

First, the simpler allocation problem was considered, where the system always is bound to move along the boundary $\Omega(G)$ without leaving it, implying that assimilate partitioning is controlled by the allometric relation at every time of year. The corresponding allocation strategy will be defined by the switching function S_Ω.

This case is approximately realized by non-seasonal tropical forests where only very small fluctuations in the driving variables, light intensity (daily averages) and temperature, occur. This implies that all input and output rate-coefficients become constant in time, simplifying the model considerably. In order to obtain a time-independent assimilation rate, the fluctuation of the function $h_1(G, I(t))$ (equation 7b) with the daily light intensity has to be eliminated. This is achieved by integration of $h_1(G, I(t))$ over 24 hours using a representative average daily light-intensity course in the tropics (see Appendix 1). As a consequence, the model equations become autonomous (the rates do not depend explicitly on time):

$$dG/dt = S_\Omega \, \bar{F}_{ASS}(G) - F_{G,efflux}(G) \tag{15}$$

$$dR/dt = (1 - S_\Omega) \, \bar{F}_{ASS}(G) - F_{R,efflux}(R) \tag{16}$$

The new, light-intensity-averaged assimilation rate is denoted by $\bar{F}_{ASS}$. Using $dR/dG = d\Omega/dG$ (the system moves only along Ω(G)), the form of the switching function for tropical forests S_Ω(G) can be obtained (see Appendix II). Inserting $S_\Omega(G)$ into (15) yields:

$$\frac{dG}{dt} = \frac{1}{1 + \dfrac{d\Omega}{dG}} \left[\bar{F}_{ASS}(G) - F_{G,efflux}(G) - F_{R,efflux}(R) \right] \tag{17a}$$

$$R = \Omega(G) \tag{17b}$$

As R is always a function of G, the differential-equation system (15), (16) reduces to one differential equation for compartment G. It can be seen that the expression in brackets from (17a) now also contains the efflux rates for the compartment R and that the growth of the G compartment is restricted by the slope of the function $\Omega(G)$: the steeper $d\Omega/dG$, the smaller dG/dt.

2.5.4. Determination of the switching function for deciduous forests

In temperate deciduous-forest ecosystems, the descriptive equations are the non-autonomous equations (13), (14). Pronounced seasonal fluctuations, especially in the leaf mass, do not permit the system to evolve strictly along the boundary curve Ω(G) as in the case of tropical, non-seasonal forests. The determination of the switching function $S_d(G)$ (d, deciduous) therefore must be extended to the entire G–R plane above $\Omega(G)$. We assume here three developmental stages during the period of one year, defined by the position of the system in the G–R plane (Fig. 2a) and each being described by a different S_d:

(1) the shooting phase, where leaf growth is preferential; $S_d(G)$ is set constant to 1 during this period and all assimilates are transferred to compartment G;
(2) the branching phase, characterized by a determinate distance Δx from the boundary $\Omega(G)$, where simultaneous build-up of leaves and wood takes place. Here, a parametrization of S_d is chosen which ensures that $\Omega(G)$ is approached continuously, while the assimilate flux into compartment R increases monotonously (see Fig. 2b and Appendix III);
(3) the secondary-growth phase, where $\Omega(G)$ is reached and the system moves along this boundary, building up new woody material and leaves according to the allometric relation, as long as favourable external conditions prevail. Here S_d is equal to S_Ω.

3. MODEL RUNS AND DISCUSSION

3.1. Tropical evergreen forests

The model with the allocation structure described in Section 2.5.3 was used to simulate a tropical broadleaved evergreen forest stand in Thailand (9° N, 99° E) as described by Kira et al. (1967). On account of the nearly constant climatic conditions, the assimilation rate was modelled by equation (A2), derived in Appendix I, choosing the parameters $I_m = 546$ W/m^2 and $L = 6$ h ($2L$ is daylength), and a constant air temperature of 27° C throughout the year for this location.

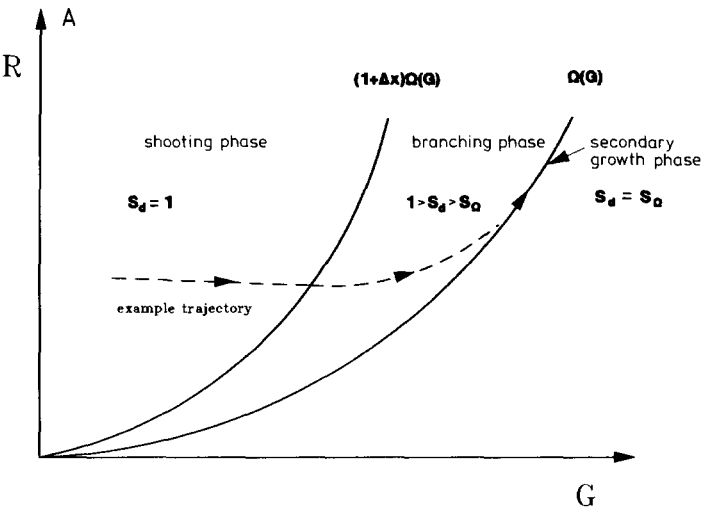

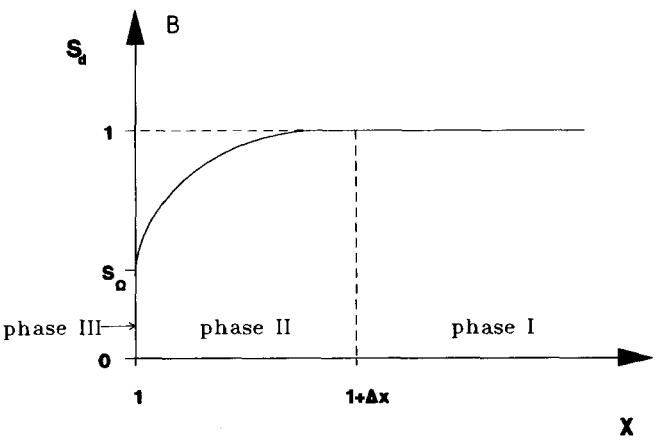

Fig. 2a. Dependence of the switching function S_d for deciduous forests on the state of the system in the $G-R$ plane.
Shooting phase: Leaf growth is preferential until the trajectory reaches a R-value which has a determinate vertical distance from the boundary $\Omega(G)$ expressed by $\Delta x\ \Omega(G)$.
Branching phase: Simultaneous build-up of leaves and wood. The phase space dependence of S_d is chosen such that the slope of the trajectory matches with the slope of $\Omega(G)$ when reaching it.
Secondary growth phase: Building up new woody material and leaves according to the allometric relation achieved by setting S_d equal to S_Ω (for the definition of S_Ω see Section 2.5.3).

Fig. 2b. Mapping of the system's state (G, R) on the variable x which describes the distance from the $\Omega(G)$ curve: I, shooting phase ($S_d = 1$); II, branching phase (S_d is parametrized as a suitably fitted ellipse segment); III, secondary growth phase ($S_d = S_\Omega$).

TABLE 2

Comparison of calculated with measured fluxes of a tropical evergreen broadleaved rainforest (Kira et al., 1967)

Mature forest ($R = 15.1$ kg C m^{-2}, $G = 1.6$ kg C m^{-2})

Annual rates $\left[\frac{\text{kg C}}{\text{m}^2 \text{ year}}\right]$	Gross photosynthetic productivity (GPP)	Respiration G-compartment	Respiration woody plant material	Leaf abscission	Woody litter
Model run	5.55	2.96	1.42	0.59	0.58
Tropical forest	5.5	2.9	1.4	0.6	0.6

In a comparison of the annual rates of carbon metabolism in the mature rain forest given by Kira et al. (1976), with the simulated values (Table 2), a fairly good agreement can be observed. Furthermore, the simulated growth curve for woody biomass R is compared with a corresponding growth-curve

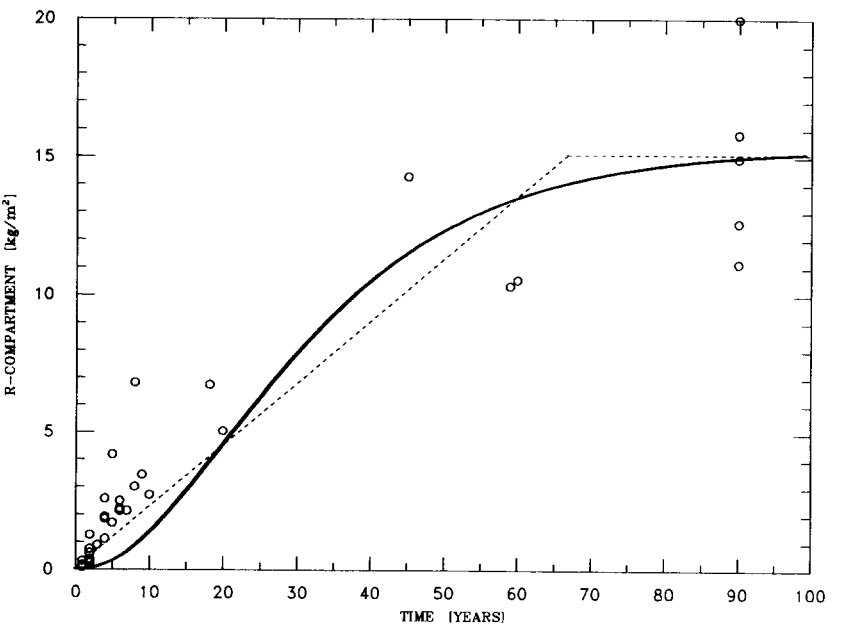

Fig. 3. Comparison of the simulated perennial carbon mass dynamics of a tropical broad-leaved evergreen forest (solid line) with biomass data from Farnworth and Golley (1974) (circles). For a better evaluation of the measured data, a regression line with the slope of 0.226 kg m^{-2} $year^{-1}$ ($\sigma = 0.315$ kg/m^2) is added (dashed line). The horizontal dashed line represents the average carbon mass in mature forests (15.1 kg/m^2).

TABLE 3

Parameters – Tropical evergreen broadleaved forest

(a) Production			
Maximum production	P_m	4.4×10^{-4}	$\frac{\text{kg C}}{\text{m}^2\ \text{h}}$
Light absorption coefficient	k	0.12	–
Conversion factor $G \rightarrow$ LAI	u	5	$\frac{\text{m}^2}{\text{kg C}}$
(b) Autotroph respiration			
Parameters defining R_R	Φ	1.55	$\frac{\text{kg C}}{\text{m}^2}$
	ψ	1.22	$\frac{\text{kg C}}{\text{m}^2}$
	γ	0.45	–
Rate coefficients			
G-compartment	a_{GA}	5.72×10^{-4}	h^{-1}
R-compartment	a_{RA}	1.88×10^{-4}	h^{-1}
(c) Litter production			
Constant rate coefficient for leaf abscission	b_{GL}	4.16×10^{-5}	h^{-1}
Litter production coefficient for R	b_{RL}	4.31×10^{-6}	h^{-1}
(d) Allometric relation $\Omega(G)$			
Constants	θ	7.2	$(\text{kg C m}^{-2})^{1/\beta}$
	β	1.58	–

derived from Farnworth and Golley (1974) (Fig. 3). The model parameter values for the tropical forest are listed in Table 3.

3.2. Deciduous forest

In model runs with the allocation strategy given by S_d, an oak forest stand in Wisconsin, U.S.A., described in the 'woodlands data set' of the International Biological Programme (Reichle, 1981), was simulated. The driving climatic variables, temperature and light intensity, were simulated in a hourly resolution using the equations given in Appendix IV; the parameters listed in Table 4 were chosen to roughly reproduce the climate at the forest site.

A set of model parameters, displayed in Table 5 has been determined from values given by Reichle (1981). In Table 6 the standing biomass and

TABLE 4

External parameters used to reproduce the climate at the forest stand in Wisconsin

Latitude	λ	44.1° N
Daily mean temperature	T_{mm}	interpolated monthly mean temperature data (Walter et al., 1975)
Mean daily temperature fluctuation	ΔT	10 K

TABLE 5

Parameters – Oak forest, Wisconsin

(a) Production			
Maximum production	P_m	1.06×10^{-3}	$\frac{\text{kg C}}{\text{m}^2\ \text{h}}$
Light absorption coefficient	k	0.1	–
Conversion factor $G \rightarrow$ LAI	u	12	$\frac{\text{m}^2}{\text{kg C}}$
(b) Autotroph respiration			
Parameters defining R_R	Φ	1.55	$\frac{\text{kg C}}{\text{m}^2}$
	ψ	1.22	$\frac{\text{kg C}}{\text{m}^2}$
	γ	0.45	–
Rate coefficients			
G-compartment	a_{GA}	4.5×10^{-3}	h^{-1}
R-compartment	a_{RA}	3.0×10^{-4}	h^{-1}
(c) Litter production			
Leaf abscission parameters	α	1×10^{-6}	h^{-1}
	ϵ	2.1	h^{-2}
	ξ	9.53	h
	b_{GL1}	1×10^{-8}	h^{-1}
Litter production coefficient for R	b_{RL}	2×10^{-6}	h^{-1}
(d) Allometric relation $\Omega(G)$			
Constants	θ	63	$(\text{kg C m}^{-2})^{1/\beta}$
	β	1.71	–

annual rates of production, respiration and litter fall, generated by the model run and integrated over the 130th year, are compared with measured annual values of the 130-year-old oak forest from Reichle (1981), showing good agreement.

TABLE 6

Comparison of calculated with measured values of an oak forest in Wisconsin (Reichle, 1981)

Age of stand: 130 years

Standing biomass	Green plant material (kg C m^{-2})	Woody plant material (kg C m^{-2})
Model run	$G/2 = 0.22$	$R = 15.7$
Wisconsin forest	0.22	16.1

Total G refers to green plant and feeder root material

Annual rates $\left[\frac{\text{kg C}}{\text{m}^2 \text{ years}}\right]$	Gross photosynthetic productivity (GPP)	Respiration green plant material	Respiration woody plant material	Leaf abscission	Woody litter
Model run	2.6	0.62	0.66	0.19	0.27
Wisconsin forest	2.3	0.51	0.50	0.22	0.22

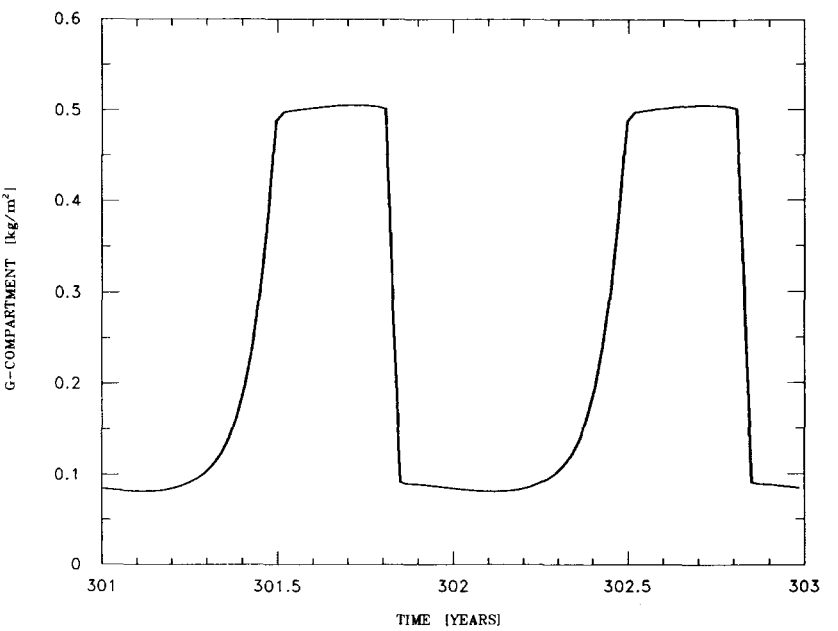

Fig. 4. Simulated seasonal fluctuations of the G-compartment (leaves, feeder roots and assimilate storage) of an oak forest near climax.

In Fig. 4 the seasonal fluctuations in carbon mass of compartment G near the climax state (in the years 301 to 303) is shown. At the beginning of the vegetation period, triggered by climate variables, the shooting of leaves and

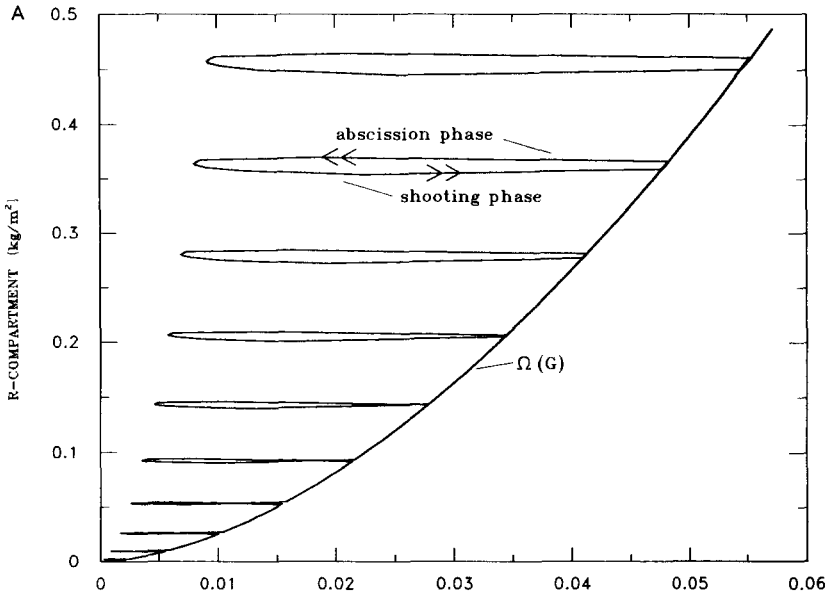

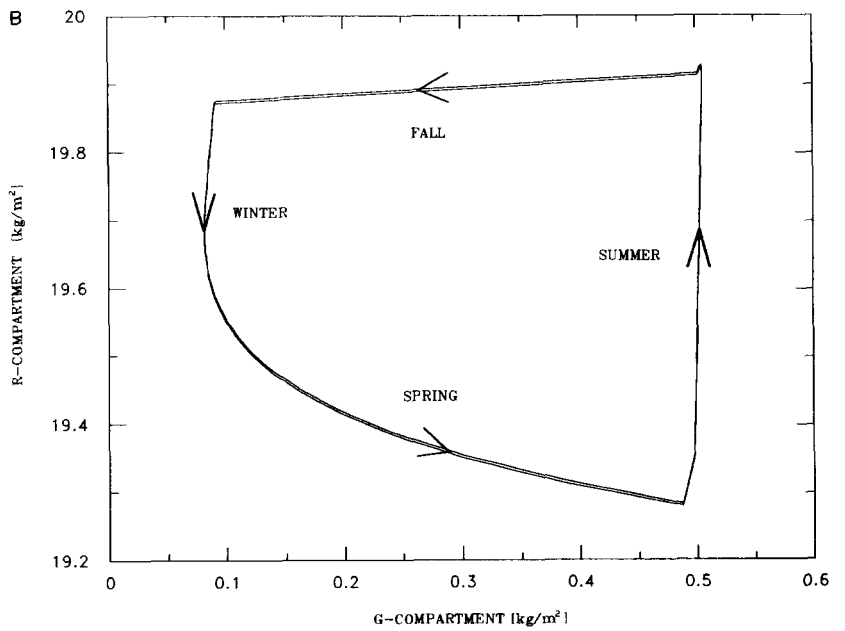

Fig. 5A. System trajectory of an oak forest in the $G-R$ plane for the first 9 years of growth. The effect of the $\Omega(G)$-boundary, the shooting and the leaf abscission phase are clearly seen.

Fig. 5B. System trajectory of an oak forest in the $G-R$ plane for 2 years near climax (the years 301 to 303). Although a strong fluctuation of biomass in the course of the year can be seen, there is no annual increment of biomass (the system reaches a limit cycle).

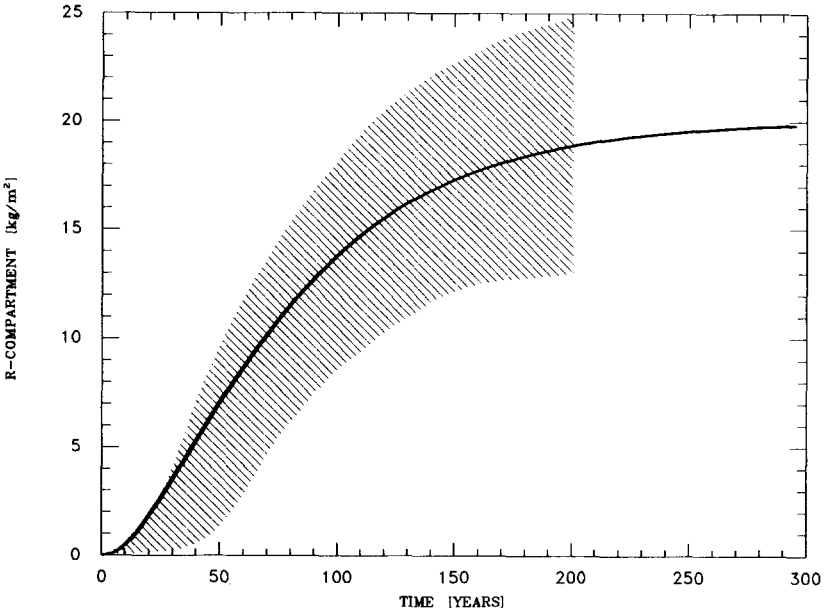

Fig. 6. Comparison of the simulated perennial carbon mass dynamics of a deciduous oak forest (solid line) with biomass data from Schober (1975). The upper and the lower boundary of the hatched area represent the highest and the lowest timber yield class, respectively.

production of feeder roots is initiated and continues until full leaf and root expansion is achieved during a time-period of one to two months, thus reproducing the correct phenology. After a maintenance period in summer, leaf abscission and corresponding feeder root death is produced, decreasing the G compartment to the remaining feeder-root quantity and assimilate-store level.

Figures 5A and B show the system trajectories in the G–R plane. Fig. 5A, displaying the first 9 years of system growth, illustrates that the simultaneous increase of the G and R compartment takes place only in the vicinity of $\Omega(G)$, representing the maximum amount of G sustained by R. In Fig. 5B, the system trajectories at the age of 301 to 303 years are plotted, showing a limit cycle.

The long-term perennial development of the woody material (compartment R) is shown in Fig. 6. About 95% of the climax biomass is reached after 300 years. Furthermore, the growth curve is compared with timber yield values for oaks in German forests (Schober, 1975), ranging between yield class I and IV.

In order to illustrate the model possibilities, another stand, a poplar forest showing quite different growth dynamics, was simulated using the same climatic input as for the Wisconsin forest. In Fig. 7 the long-term growth of compartment R, reaching 95% of the climax state already in 60 years, is

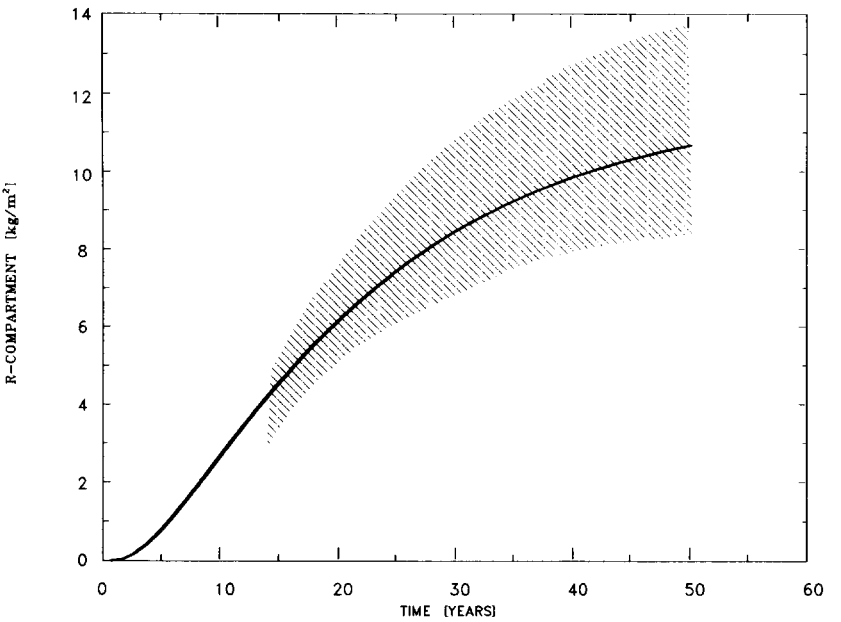

Fig. 7. Comparison of the simulated perennial carbon mass dynamics of a deciduous poplar forest (solid line) with biomass data from Schober (1975). The upper and lower boundary of the hatched area represent the highest and the lowest timber yield class, respectively.

compared to German poplar yield data from Schober (1975). The corresponding parameter set is given in Table 7.

CONCLUSIONS

Based on a two-compartment structure of the living biomass, here G (photosynthesizing tissue, feeder roots and assimilate store) and R (remaining woody biomass), both seasonal and perennial carbon dynamics of deciduous type forests could be modelled in dependence of the biomass state and climatic variables. The central part of the model consists of an allocator in form of the switching function S, which distributes the assimilates to the compartments G and R, solely on consideration of the the phase-space G/R and climatic variables, renouncing to prescribe the time-course of the phenophases explicitely (phase-space control). In the first approach model, only light intensity and temperature as external variables have been considered. Comparison of the model runs with available experimental data indicates that a successful description of other ecosystem types should be possible with a similar model structure.

The model requires a number of vegetation type-specific parameters, which, however, constitute measurable quantities with a known value, or at

TABLE 7

Parameters – Poplar stand in Wisconsin

(a) Production			
Maximum production	P_m	1.06×10^{-3}	$\frac{\text{kg C}}{\text{m}^2\ \text{h}}$
Light absorption coefficient	k	0.1	–
Conversion factor G → LAI	u	15	$\frac{\text{m}^2}{\text{kg C}}$
(b) Autotroph respiration			
Parameters defining R_R	Φ	3.58	$\frac{\text{kg C}}{\text{m}^2}$
	ψ	2.15	$\frac{\text{kg C}}{\text{m}^2}$
	γ	0.60	–
Rate coefficients			
G-compartment	a_{GA}	4.5×10^{-3}	h^{-1}
R-compartment	a_{RA}	5.7×10^{-4}	h^{-1}
(c) Litter production			
Leaf abscission parameters	α	1×10^{-6}	h^{-1}
	ϵ	2.1	h^{-2}
	ξ	9.53	h
	b_{GL1}	1×10^{-8}	h^{-1}
Litter production coefficient for R	b_{RL}	1.2×10^{-6}	h^{-1}
(d) Allometric relation $\Omega(G)$			
Constants	θ	81	$(\text{kg C m}^{-2})^{1/\beta}$
	β	2	–

least its possible range. Global-coverage vegetation data in a seasonal time resolution offer a powerful tool for further model verification in future. Thus, extending the model by a precipitation and nutrient dependence, a reasonable modeling of the vegetation response to climatic variations at any point of the world could become feasible. Then the feed-back effects between vegetation and a future greenhouse climate can be studied on different levels of complexity, as only three climatic variables are required as model input.

By incorporating a dead-biomass decomposition submodel and accounting for the dependence of the assimilation rate on ambient CO_2, the model may also be integrated into more-complex models of the global carbon cycle, allowing for detailed seasonal simulations and a comparison with measured seasonal atmospheric CO_2 variations.

ACKNOWLEDGEMENTS

The authors thank the Bundesministerium für Forschung und Technologie for financial support. The technical assistance of Olaf Timpe is gratefully acknowledged.

APPENDIX I

Integration of the function h_1, describing the instantaneous photosynthesis rate as a function of light intensity $I(t)$ during the course of 24 h

(1) Approximation of the daily light-intensity function $I(t)$ in order to allow for analytical treatment:

$$I(t) = -I_m \frac{1}{L^2}(t - t_a)(t - t_e) \tag{A1}$$

with

$$L = \tfrac{1}{2}(t_a - t_e)$$

where I_m maximum light intensity, t_a time of sunrise, t_e time of sunset, and $2L$ daylength.

It can be shown numerically that the proposed parabola is a fair approximation of the real daily light-intensity course.

(2) Integration:

$$\int_0^{24} h_1(G, I(t))\,\mathrm{d}t$$

$$= \frac{2P_m L}{k}\left[(V_1+1)\left[\ln(L(V_1+1))-1\right] - (V_1-1)\left[\ln(L(V_1-1))-1\right]\right.$$

$$\left. -(V_2+1)\left[\ln(L(V_2+1))-1\right] + (V_2-1)\left[\ln(L(V_2-1))-1\right] - kuG\right] \tag{A2}$$

with

$$V_1 = \sqrt{1 + \frac{K_I}{I_m}}$$

and

$$V_2 = \sqrt{1 + \frac{K_I}{I_m\, e^{-kuG}}}$$

where K_I is the Michaelis–Menten constant for light intensity, k extinction

coefficient, G carbon mass of the G compartment, and u conversion factor $G \rightarrow$ leaf area index LAI.

If, in the tropics, L and I_m are assumed to be constant during the course of the year, the carbon assimilation rate (equation A2) becomes dependent only on the variable G.

APPENDIX II

Determination of the switching function S_Ω in tropical evergreen forests

From equations (13), (14) follows the slope of the trajectory:

$$\frac{dR}{dG} = \frac{(1 - S_\Omega)\bar{F}_{ass}(G) - F_{R,efflux}(R)}{S_\Omega \bar{F}_{ass}(G) - F_{G,efflux}(G)} \tag{A3}$$

Since at any time R and G are related by the allometry constraint:

$$\frac{dR}{dG} = \frac{d\Omega}{dG} \tag{A4}$$

equation (A3) can be solved for S_Ω:

$$S_\Omega(G) = \frac{\bar{F}_{ass}(G) + \frac{d\Omega}{dG} F_{G,efflux} - F_{R,efflux}(\Omega(G))}{\left[1 + \frac{d\Omega}{dG}\right] \bar{F}_{ass}(G)} \tag{A5}$$

APPENDIX III

Parametrization of the switching function S_d for temperate deciduous forests

As a measure of the position in the G–R plane the ratio x between the actual value of $R(t)$ and its corresponding 'equilibrium value', described by $\Omega(G)$, is defined:

$$x = R(t)/\Omega(G) \qquad \text{with} \quad x \geqslant 1 \tag{A6}$$

In Fig. 2b the course of S_d in the three different phases, characterized by the situation of the system point in the G–R plane is shown:

(1) shooting phase (I)

for $x \geqslant (1 + \Delta x)$

$S_d = 1$

(2) branching phase (II)

for $1 < x < (1 + \Delta x)$

S_d is parametrized as an ellipse segment, determined by following conditions:

$$S_d(1 + \Delta x) = 1 \tag{A7a}$$

$$\left.\frac{dS_d}{dx}\right|_{1+\Delta x} = 0 \tag{A7b}$$

$$S_d(1) = S_\Omega(G, t) \tag{A7c}$$

$$\left.\frac{dS_d}{dx}\right|_{1} = \infty \tag{A7d}$$

(3) secondary growth phase (III)

for $x = 1$

$S_d = S_\Omega$

APPENDIX IV

Simulation of the driving variables temperature and light intensity as a function of time

In the model year, 360 days with 12 months @ 30 days have been assumed.

Air temperature:

$$T(t) = T(t_d, t_h) = T_{mm}(t_d) + \Delta T/2 \cos\left(\pi \frac{t_h - 14}{12}\right) \tag{A8}$$

Light intensity (Richter, 1985):

$$I(t) = I(t_d, t_h) = \begin{cases} I_{max}\, I^*(t) \exp(-k_{atm}/I^*(t)) & \text{if} \quad I^*(t) \geqslant 0 \\ 0 & \text{otherwise} \end{cases} \tag{A9a}$$

$$I^*(t) = I(t_d, t_h) = \sin\lambda \sin\delta + \cos\lambda \cos\delta \cos\left(\pi \frac{t_h - 12}{12}\right) \tag{A9b}$$

$$\delta(t) = \delta(t_d) = -0.408 \cos\left(\pi \frac{t_d + 10}{180}\right) \tag{A9c}$$

Daylength:

$$D(t) = D(t_d) = \frac{24}{\pi} \arccos[-\tan\lambda \tan\delta(t_d)] \tag{A10}$$

t_h	daytime in hours
t_d	day number
$T_{mm}(t_d)$	daily averaged values obtained from temperature records
ΔT	average daily temperature fluctuation
λ	geographical latitude
I_{max}	maximum intensity of PAR = 640 W/m^2
δ	sun declination
k_{atm}	atmospheric absorption coefficient

REFERENCES

Bertalanffy, L., Beier, W. and Laue, R., 1977. Biophysik des Fließgleichgewichts. Vieweg, Braunschweig, 157 pp.

Čestnych, O.V. and Gil'manov, T.G., 1986. Matematičeskaja model' sezonnoj fenologičeskoj dinamiki eli v ekosistemach južnoj tajgi (Mathematical model of seasonal phenological dynamics of spruce in southern taiga ecosystems). Vestn. Mosk. Univ. Ser. 16 Biol., 1: 65–73 (in Russian).

Esser, G., 1989. Stoffhaushalt landwirtschaftlicher Intensivkulturen im Rahmen von LOTREX 10E/HIBE 88 (LOF 37/87). Klimaforschungsprogramm, Statusseminar, 10–12 January 1989, Gesellschaft für Strahlen- und Umweltforschung, Hamburg. Preconference Volume, pp. 155–158.

Farnworth & Golley, 1974. Fragile Ecosystems. Springer, New York.

Fung, I.Y., Tucker, C.J. and Prentice, K.C., 1987. Application of advanced very high resolution radiometer vegetation index to study atmosphere–biosphere exchange of CO_2. J. Geophys. Res., D3: 2999–3015.

Gates, D.M., 1980. Biophysical Ecology. Springer, New York.

Johnson, F.H., Eyring, H. and Polissar, M.J., 1954. The Kinematic Basis of Molecular Biology. Wiley, New York.

King, A.W., DeAngelis, D.L. and Post, W.M., 1987. The seasonal exchange of carbon dioxide between the atmosphere and the terrestrial biosphere: extrapolation from site-specific models to regional models. ORNL/TM-10570, available from NTIS, U.S. Department of Commerce, Springfield, VA.

Kira, T., Ogawa, H., Yoda, K. and Ogino, K., 1967. Comparative ecological studies on three main types of forest vegetation in Thailand. Nat. Life, 5: 146–174.

Kohlmaier, G.H., Bröhl, H., Siré, E.O., Plöchl, M. and Revelle, R., 1987. Modelling stimulation of plants and ecosystem response to present levels of excess atmospheric CO_2. Tellus, 39B: 155–170.

Lommen, P.W., Schwintzer, C.R., Yocum, C.S. and Gates, D.M., 1971. A model discribing photosynthesis in terms of gas diffusion and enzym kinetics. Planta, 98: 195–220.

Mitscherlich, G., 1975. Wald, Wachstum und Umwelt, III. Sauerländer, Frankfurt, 352 pp.

Monsi, M. and Saeki, T., 1953. Über den Lichfaktor in Pflanzengesellschaften und seine Bedeutung für die Stoffproduktion. Jpn. J. Bot., 14: 22–52.

Oikawa, T., 1985. Simulation of forest carbon dynamics based on a dry-matter production model. I. Fundamental model structure of a tropical rainforest ecosystem. Bot. Mag. Tokyo, 98: 225–238.

Pearman, G. and Hyson, P., 1986. Global transport and inter-reservoir exchange of carbon dioxide with particular reference to stable isotopic distributions. J. Atmos. Chem., 1: 81–124.

Reichle, D.E., 1981. Dynamic Properties of Forest Ecosystems. IBP, 23. Cambridge University Press, Cambridge, 663 pp.

Richter, O., 1985. Simulation des Verhaltens ökologischer Systeme – Mathematische Methoden und Modelle. VHC, Weinheim, 219 pp.

Rosen, R., 1967. Optimality Priciples in Biology. Butterworth, London.

Schober, R., 1975. Ertragstafeln Wichtiger Baumarten. Sauerländer, Frankfurt.

Solomon, A.M., 1986. Transient response of forests to CO_2-induced climate change: simulation modeling experiments in eastern North America. Oecologia, 68: 567–579.

Strasburger, E., 1985. Lehrbuch der Botanik. Fischer, Stuttgart, 1078 pp.

Walter, H., Harnickell, E. and Mueller-Dombois, D., 1975. Klimadiagramm-Karten der einzelnen Kontinente und die ökologische Klimagliederung der Erde. Fischer, Stuttgart.